LIMNOLOGY and OCEANOGRAPHY

ASLO

Limnol. Oceanogr. 9999, 2021, 1–17

doi: 10.1002/lno.11786

Unexpected shift from phytoplankton to periphyton in eutrophic streams due to wastewater influx

Nathanael T. Bergbusch,[1,2] **Nicole M. Hayes**,[1,2,a] **Gavin L. Simpson**,[2] **Peter R. Leavitt**[1,2,3*]

[1]Limnology Laboratory, Department of Biology, University of Regina, Regina, Saskatchewan, Canada
[2]Institute of Environmental Change and Society, University of Regina, Regina, Saskatchewan, Canada
[3]Institute for Global Food Security, Queen's University Belfast, Belfast, UK

Abstract

Pollution with nitrogen (N) and phosphorous (P) impairs streams by favoring suspended algae and cyanobacteria over diatom-rich periphyton. Recently, wastewater treatment plants have been upgraded to biological nutrient removal to eliminate both P and N (mainly NH_4^+), although little is known of the effects of this effluent on flowing waters. Here, we used high performance liquid chromatography to quantify how the abundance and composition of phytoplankton and periphyton varied in response to both influx of effluent produced by biological nutrient removal and physico-chemical conditions in small, turbid, P-rich streams of the northern Great Plains. At the catchment scale, analysis with generalized additive models (GAMs) explained 40.5–62.6% of deviance in total phototroph abundance (as Chl *a*) and 72.5–82.5% of deviance in community composition (as biomarker carotenoids) in both planktonic and benthic habitats when date- and site-specific physico-chemical parameters were used as predictors. In contrast, GAMs using wastewater input (as aqueous $\delta^{15}N$) as a predictor explained up to 50% of deviance in Chl *a*, and ~60% of deviance in community composition, in both suspended (51.6% of Chl *a*, 67.1% of composition) and attached communities (21.5% of Chl *a*, 58.8% of composition). Phytoplankton was replaced by periphyton within a 60-km wastewater-impacted reach due to dilution of streams by transparent effluent and addition of urban NO_3^-, although predominance of phytoplankton was re-established after confluence with higher-order streams. Overall, influx of effluent shifted turbid, phytoplankton-rich streams to clear ecosystems with abundant epilithon by improving water transparency and providing NO_3^- to favor benthic diatoms and chlorophytes.

Nutrient-rich discharge from urban wastewater treatment plants degrades freshwaters in streams and rivers by causing eutrophication (Holeton et al. 2011) and promoting harmful levels of algae and cyanobacteria (Dodds and Smith 2017; Hamdhani et al. 2020). Alongside nutrient effects, wastewater treatment plant effluent can also affect phototrophic communities in flowing waters by modifying hydrological discharge, thermal characteristics, and irradiance regimes (Carey and Migliaccio 2009; Holeton et al. 2011). While effects of urban effluent on primary production, as well as primary producer biomass and composition, in rivers and streams has been generally well studied (Murdock et al. 2004; Gücker et al. 2006; Waiser et al. 2011), less is known of how the effects of effluent may change the importance of phytoplankton or periphyton communities in space and time (Hamdhani et al. 2020). Further, prior research has typically investigated impacts of secondary- (low dissolved organic matter, DOM; high nutrients) or tertiary-treated effluent (low DOM; low P, high N) on flowing waters (Carey and Migliaccio 2009), and less is known of the effect of modern wastewater treatment processes, such as biological nutrient removal, which produces effluent with low content of DOM, N and P (Carey and Migliaccio 2009; Hamdhani et al. 2020).

Management of urban wastewaters has undergone substantial development during the past 50 yr (Tchobanoglous et al. 2003; Carey and Migliaccio 2009). Following experimental evidence that pollution with P caused widespread eutrophication of freshwaters (Schindler 1977; Dodds and Smith 2017), many inland urban centers upgraded wastewater treatment plants in the 1970s to remove P by chemical precipitation, usually as insoluble ferric compounds (Tchobanoglous et al. 2003). However, tertiary treatment does not eliminate

*Correspondence: peter.leavitt@uregina.ca, p.leavitt@qub.ac.uk

Additional Supporting Information may be found in the online version of this article.

[a]Present address: Biology Department, University of Wisconsin Stout, Menomonie, Wisconsin, USA

inorganic N, and toxic levels (40 mg N–NH_4^+ L^{-1}) of ammonium (NH_4^+) in effluent (Waiser et al. 2011; others) can depress stream production (Waiser et al. 2011), while also favoring toxic cyanobacteria (Donald et al. 2011; Solomon et al. 2019). To address this issue, biological nutrient removal technologies were developed that use sequential microbial nitrification, denitrification, and nutrient uptake to reduce total N by up to 95%, largely eliminate NH_4^+, and release only moderate levels of NO_3^- (<5 mg N-NO_3^- L^{-1}) and P (<1 mg P-PO_4^{3-} L^{-1}) to surface waters (Carey and Migliaccio 2009). However, while elimination of NH_4^+ toxicity is environmentally desirable, many cities have yet to upgrade their facilities to biological nutrient removal processes (Organization for Economic Cooperation and Development 2020), possibly due to high costs of new facilities (>$100 million per treatment plant; Environmental Protection Agency 2007) and the relative paucity of research on the effects of this new N-depleted effluent on freshwaters (Schindler et al. 2016).

Effluent from biological nutrient removal is expected to interact with in situ physico-chemical features of flowing waters to regulate both planktonic and benthic primary producers in complex manners that vary in time and space (Dodds et al. 2006; Wu et al. 2011; Breuer et al. 2017). Excess nutrients promote phototroph blooms (Chambers et al. 2012; Dodds and Smith 2017), as well as changes in community composition (Glibert et al. 2016) and habitat of production (Roeder 1977; Wu et al. 2011; Breuer et al. 2017), with benthic diatoms giving way to chlorophytes and cyanobacteria in suspended (Mischke et al. 2011) and benthic communities (Peterson and Grimm 1992; McCall et al. 2017). However, nutrient effects should also depend on baseline production and stoichiometry of streams, as low N:P ratios may favor harmful cyanobacteria (Dodds and Smith 2017), while changes in individual chemical forms (e.g., NO_3^- vs. NH_4^+) can exert taxon-specific effects on algae (Glibert et al. 2016; Solomon et al. 2019; Kim et al. 2020). Although irradiance regimes affect both suspended and attached phototrophs in flowing waters (Munn et al. 1989; Hutchins et al. 2010), effects of photon flux vary seasonally with discharge and turbidity (Biggs 1995; Leland 2003), canopy cover (Rosemond et al. 2000), nutrient content (Glibert et al. 2016), and temperature (Baker and Baker 1979; Munn et al. 2002; Wu et al. 2011). Such seasonal changes also drive patterns of benthic and suspended community development (Andrus et al. 2015), with enhanced production of diatoms in spring and fall and elevated densities of chlorophytes and cyanobacteria in summer (Breuer et al. 2016; Moorhouse et al. 2018). Overall, the degree to which natural phototrophic phenology interacts with effluent influx is poorly understood (del Giorgio et al. 1991; Stevenson and White 1995; Solomon et al. 2019), particularly for streams in nonboreal systems such as agricultural grasslands (Dodds et al. 2004; Breuer et al. 2017).

This paper uses generalized additive models (GAMs) to analyze how spatial and temporal variation in physical and chemical parameters interacts with effluent from biological nutrient removal to regulate abundance and composition of periphyton and phytoplankton in two prairie streams. Study systems are P-rich, turbid, low-order grassland streams, one of which receives urban wastewater mid-reach. Phototrophic communities were quantified using taxonomically diagnostic pigment biomarkers (chlorophylls [Chl], carotenoids) to measure: (1) how regional variation in physico-chemical conditions affected development of phototrophic biomass and community composition; (2) how modern effluent affected phytoplankton and periphyton; and (3) whether urban effluent had a differential effect on suspended or attached communities. We hypothesized that: (1) landscape patterns of abundance, composition and interaction of phytoplankton and periphyton would reflect spatial and temporal variation in regulation by physico-chemical parameters (discharge, irradiance, temperature) in these eutrophic streams (Breuer et al. 2016, 2017; Moorhouse et al. 2018); (2) effluent influx would overwhelm natural landscape controls (discharge, irradiance, temperature) of periphyton (Murdock et al. 2004; Hamdhani et al. 2020) and phytoplankton development (del Giorgio et al. 1991; Stevenson and White 1995; Solomon et al. 2019); (3) modern urban effluent would favor phytoplankton over periphyton due to both changes in nutrient (Chambers et al. 2012; Dodds and Smith 2017) and irradiance regimes (Munn et al. 1989; Rosemond et al. 2000); and (4) NO_3^- from effluent would favor siliceous algae and chlorophytes over cyanobacteria downstream of wastewater treatment plant outfall (Glibert et al. 2016; Swarbrick et al. 2019).

Methods

Study area

Study sites consisted of first-order Wascana Creek and higher-order Qu'Appelle River, small grassland streams within the Prairies of southern Saskatchewan, Canada (Fig. 1 and Table 1). The Qu'Appelle River drainage basin covers ~52,000 km^2 of intensive agriculture (mainly wheat, canola) and more limited natural grassland, wetland, and urban environments (Hall et al. 1999). Regional climate is a cool-summer humid continental regime (Köppen D*fb*), with high seasonal variation, short summers (July mean of 19°C), cold winters (January mean of −16°C), and low-annual temperatures (~1.5°C) (Leavitt et al. 2006; Swarbrick et al. 2020). Wascana Creek is a naturally intermittent prairie stream draining ~1400 km^2 in a northwest direction through Wascana Lake and the City of Regina, before receiving treated effluent from a wastewater facility using biological nutrient removal (Fig. 1). Wascana Creek continues northwest ~60 km before its confluence with the Qu'Appelle River, a larger stream flowing east to Pasqua Lake (Leavitt et al. 2006). The Qu'Appelle River originates in wetlands near Eyebrow Lake west of Regina and flows eastward though eutrophic Buffalo Pound Lake before its confluence with Wascana Creek (Fig. 1). Flow in the Qu'Appelle River is also supplemented year-round by water discharged from the mesotrophic Lake Diefenbaker reservoir and, in late

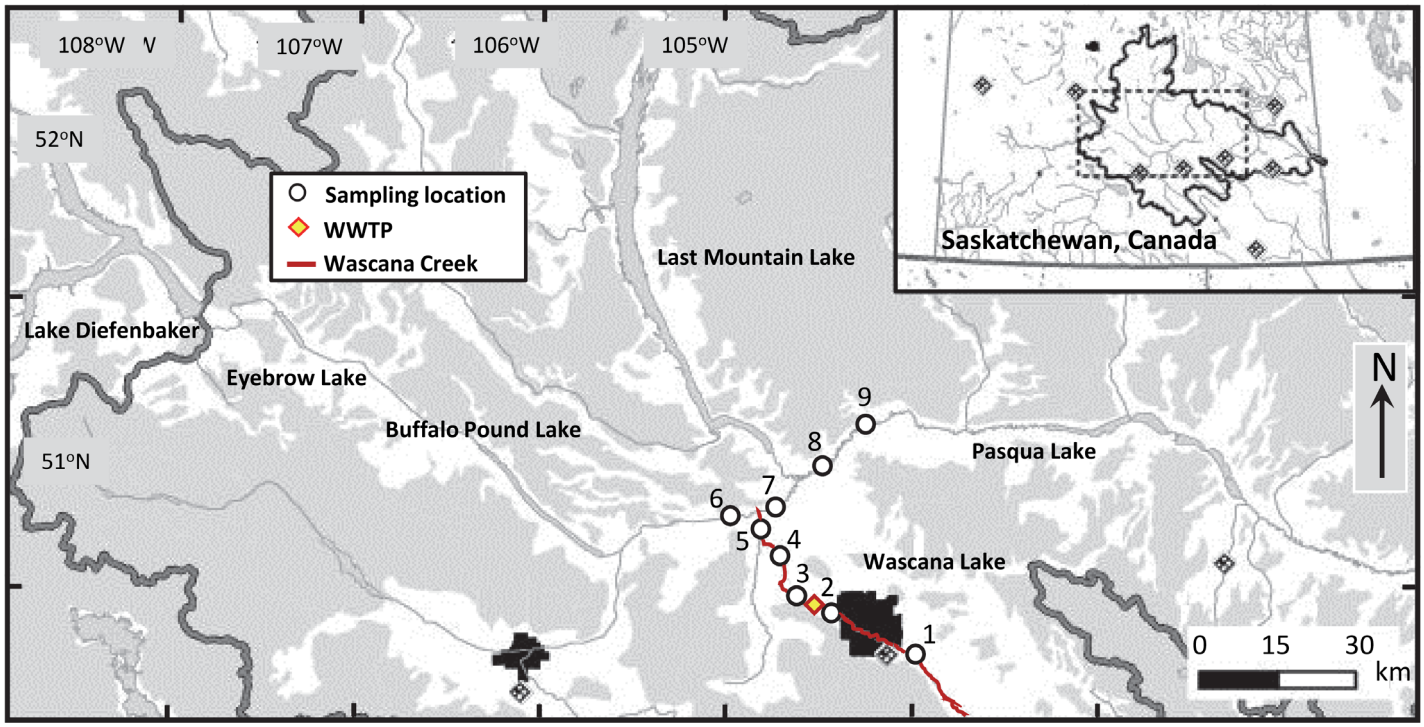

Fig 1. Map of sampling sites within Wascana Creek (1–5) and the Qu'Appelle River (6–9) in Saskatchewan, Canada (SK, upper right). Wascana Creek in red, sampling locations as white circles, and City of Regina (black square) wastewater treatment plant as yellow diamond.

summer of most years, by flow from eutrophic, sub-saline Last Mountain Lake immediately northeast of the Wascana Creek-Qu'Appelle River confluence. Catchment hydrology is detailed in Haig et al. (2020).

Both Wascana Creek and Qu'Appelle River are naturally small, turbid, alkaline, and P-rich streams, often exhibiting N limitation and abundant suspended cyanobacteria by late summer (Waiser et al. 2011; Supporting Information Fig. S1). Discharge in both systems is highly seasonal, with spring snow melt accounting for 80% of surface runoff (Pham et al. 2009; Haig et al. 2020). Flow is limited during winter and much of summer, particularly in Wascana Creek where effluent from the wastewater treatment plant makes up most of the discharge during June to September and November to March (Waiser et al. 2011). Presently, mean (± SE) effluent nutrient levels include 5.8 ± 0.07 mg N L^{-1} as NO_3^-, 1.82 ± 0.07 mg N L^{-1} as NH_4^+, and 0.58 ± 0.02 mg P L^{-1} as TDP (Table 1).

Field methods

Nine stations were sampled along the continuum formed from Wascana Creek headwaters to Qu'Appelle River near Pasqua Lake (Fig. 1), including two sites upstream of the wastewater treatment plant outfall (before and after Wascana Lake), three stations between the outfall and the Wascana - Creek-Qu'Appelle River confluence, and four locations along the mainstem of the Qu'Appelle River (upstream of confluence, upstream of Last Mountain Lake inflow, two further downstream). All sites were sampled every 2 weeks 1 May to 15 September 2018 and 2019 between 9:00 and 14:00 h. At each station, temperature (°C), cloud cover (%), and wind velocity (km s^{-1}) were recorded, while a YSI Model 85 m was used to register water temperature (°C), dissolved oxygen (mg O_2 L^{-1}), specific conductivity (μS cm^{-1}), salinity (g total dissolved solids [TDS] L^{-1}), and pH at surface, mid-column, and near-bottom depths. Surface values were used for subsequent analyses, as there was limited variation with water-column position. Water transparency was recorded with a 20-cm diameter Secchi disk, as well as a LaMotte model 2020we turbidity meter.

On each date, a 10-L sample of water was obtained from the stream center at each site by integrating discrete samples collected from surface to mid-column depths. Water was screened though a 243-μm pore mesh to remove invertebrates and particulate matter, but not phytoplankton (Vogt et al. 2018). Periphyton samples at each location were collected from the stream side at ~12 ± 2 cm depth by brushing three similar-sized biofilms of known area (~5 cm diameter) from rocks randomly chosen from a geo-referenced cobble deposit. We selected this depth as it represented ~50% of Secchi depth in the turbid reaches of the study system. Rather than let sampling depth vary with water-column transparency (e.g., storm events), we selected a fixed sampling depth to quantify a representative epilithic response.

Table 1. The spatial physico-chemical values (mean ± SE) at each stream location and the wastewater treatment plant (WWTP) effluent from May to September in 2018 and 2019. Note that effluent turbidity is the mean and SE of measurements during 2017 as turbidity was not recorded in 2018 or 2019. Site 6 is an additional site on the Qu'Appelle River upstream of the confluence of Wascana Creek and Qu'Appelle River. Salinity is in g total dissolved solids L^{-1}. Sp. cond. is specific conductivity. Nutrients include total dissolved nitrogen (TDN), nitrate (NO_3^-), ammonium (NH_4^+), total dissolved phosphorus (TDP), soluble reactive phosphorus (SRP), and stable isotope values of filtered water or effluent ($\delta^{15}N$).

Site	1	2	3	4	5	6	7	8	9	WWTP
Distance to WWTP (km)	−43	−7	4	36	60	—	69	104	137	0
Maximum depth (cm)	97.89 ± 3.21	98.84 ± 2.69	67.50 ± 2.43	86.53 ± 3.85	88.72 ± 2.69	120.28 ± 2.92	100.03 ± 3.54	102.64 ± 1.40	73.75 ± 1.59	—
Discharge ($m^3 s^{-1}$)	0.06 ± 0.03	0.58 ± 0.24	1.18 ± 0.21	1.34 ± 0.32	1.42 ± 0.52	3.08 ± 0.81	4.29 ± 0.88	2.90 ± 0.17	3.68 ± 0.17	0.81 ± 0.01
Turbidity (NTU)	4.97 ± 0.54	24.33 ± 2.32	7.39 ± 1.08	12.52 ± 2.53	18.51 ± 4.39	38.30 ± 3.99	32.98 ± 4.55	30.99 ± 3.83	40.03 ± 4.60	4.45 ± 0.27
Secchi (cm)	63.35 ± 7.59	20.04 ± 1.31	53.46 ± 2.99	50.68 ± 5.27	37.66 ± 4.13	16.94 ± 1.08	21.69 ± 1.60	19.86 ± 2.11	17.83 ± 3.04	—
pH	8.60 ± 0.13	8.42 ± 0.08	7.77 ± 0.06	8.84 ± 0.10	8.66 ± 0.09	8.49 ± 0.06	8.52 ± 0.05	8.61 ± 0.09	8.77 ± 0.07	7.42 ± 0.01
Salinity ($g L^{-1}$)	1.03 ± 0.05	0.45 ± 0.02	0.72 ± 0.04	0.71 ± 0.04	0.75 ± 0.03	0.38 ± 0.02	0.51 ± 0.04	0.60 ± 0.05	0.58 ± 0.05	—
Sp. cond. ($\mu S\ cm^{-1}$)	1999.55 ± 82.07	910.49 ± 48.54	1436.00 ± 62.43	1412.29 ± 80.95	1468.30 ± 65.59	757.34 ± 40.45	1055.35 ± 78.43	1203.30 ± 100.34	1182.80 ± 90.24	—
Temperature (°C)	16.88 ± 0.82	17.49 ± 0.84	17.95 ± 0.70	18.75 ± 0.80	18.16 ± 0.85	18.06 ± 0.81	18.28 ± 0.83	17.83 ± 0.78	17.56 ± 0.78	20.07 ± 0.14
TDN ($mg N L^{-1}$)	1.75 ± 0.14	0.99 ± 0.06	5.53 ± 0.52	3.19 ± 0.42	2.83 ± 0.40	0.62 ± 0.04	1.52 ± 0.30	1.00 ± 0.11	0.93 ± 0.09	10.62 ± 0.12
NO_3^- ($mg N L^{-1}$)	0.02 ± 0.01	0.05 ± 0.01	1.88 ± 0.24	1.21 ± 0.25	1.02 ± 0.24	0.02 ± 0.01	0.38 ± 0.10	0.12 ± 0.04	0.04 ± 0.01	5.80 ± 0.07
NH_4^+ ($mg N L^{-1}$)	0.03 ± 0.01	0.11 ± 0.03	0.89 ± 0.21	0.11 ± 0.03	0.14 ± 0.09	0.05 ± 0.03	0.04 ± 0.01	0.06 ± 0.03	0.06 ± 0.03	1.82 ± 0.07
$\delta^{15}N$ (‰)	4.93 ± 0.28	5.73 ± 0.66	15.22 ± 0.73	13.63 ± 0.78	13.97 ± 1.04	5.26 ± 0.84	11.00 ± 1.02	7.61 ± 0.50	6.27 ± 0.41	16.82 ± 0.28
TDP ($mg P L^{-1}$)	0.38 ± 0.07	0.09 ± 0.01	0.21 ± 0.04	0.12 ± 0.01	0.13 ± 0.01	0.04 ± 0.01	0.08 ± 0.01	0.05 ± 0.01	0.04 ± 0.01	0.58 ± 0.02
SRP ($mg P L^{-1}$)	0.25 ± 0.05	0.05 ± 0.01	0.08 ± 0.01	0.065 ± 0.01	0.07 ± 0.01	0.03 ± 0.01	0.05 ± 0.01	0.03 ± 0.01	0.02 ± 0.01	—
TDN:SRP	13.78 ± 2.68	37.83 ± 8.29	79.85 ± 11.22	86.85 ± 26.67	74.10 ± 16.46	45.31 ± 5.72	55.95 ± 10.99	59.70 ± 8.52	65.94 ± 12.15	—

Periphyton samples were diluted with deionized water and stored in Whirl-Pak® bags for transportation. Although subject to potentially greater variability (Morin and Cattaneo 1992), we used natural substrates to both better capture the normal phenology of epilithon, and to avoid the underestimation of total periphyton, chlorophyte, and cyanobacteria abundances commonly associated with use of artificial surfaces (Cattaneo and Amireault 1992). We measured instantaneous water velocity, water-column depth, and channel cross-sectional area at wade-able sites (<1.2 m depth) using a calibrated Swoffer Instruments Inc. model 2100 current velocity meter, following the two-point (>0.75 m) and 6/10th (<0.75m) depth methods of Buchanan and Somers (1976) as detailed in Swarbrick (2017). All samples were processed in the laboratory on day of collection. In addition, we collected weekly discrete (instantaneous) and 24-h integrated samples of final urban effluent from EPCOR Utilities for the period of May 2018 to August 2019.

Laboratory methods

Whole-water and periphyton samples were filtered through GF/C glass fiber filters (1.2 μm nominal pore size) and stored frozen at −20°C until later analysis of pigments and stable isotopes. Filtrate was then passed through 0.45-μm pore membrane filters and frozen at −20°C until analysis of dissolved nutrients. GF/C filters were used for pigment and isotope analyses.

Concentrations of ammonia (NH_3) /ammonium (hereafter as NH_4^+), nitrite (NO_2^-) /nitrate (hereafter as NO_3^-), total dissolved nitrogen (TDN), SRP, and total dissolved phosphorous (TDP) were analyzed using a Lachat QuikChem 8500 FIA automated ion analyzer and standard procedures (APHA-AWWA/WEF 1998). In addition, the City of Regina supplied monthly estimates of NH_4^+, NO_2^-, NO_3^-, TDN, and TDP collected near our sites, as well as at additional locations. Finally, nutrient concentrations in treated effluent from the Regina wastewater treatment plant were supplied by EPCOR Utilities (Edmonton, Canada). All N and P species were expressed as mg nutrient L^{-1}.

Stable isotopes of carbon (C) and N from filtered water, effluent, particulate organic matter (POM, mainly phytoplankton), and periphyton were measured for all sampling sites to estimate fluxes of ^{15}N-enriched effluent (22–25 ‰ in summer) following Leavitt et al. (2006). Briefly, GF/C-filtered water and effluent samples were freeze-dried (1 week, 0.01 Pa) to obtain residue for analysis, whereas POM and periphyton filters were dried in an oven at 66°C for 24 h. To optimize N analyses, we packed 10–15 mg of solids from treated effluent or wastewater-impacted river sites, whereas 20–25 mg was used for isotope analysis of undisturbed sites. We used six 6-mm diameter hole-punches of GF/C filters for stable isotope analysis of POM and periphyton. All solids were folded into individual tin capsules and combusted in a NC2500 Elemental Analyzer (ThermoQuest, CE Instruments) coupled to a

Thermoquest (Finnigan-MAT) Delta PlusXL isotope ratio mass spectrometer (IRMS). Stable isotope values are presented using standard expressions ($\delta^{13}C$, $\delta^{15}N$) calibrated relative to atmospheric and laboratory standards, whereas elemental content was expressed as % dry mass (% C, % N).

Total abundance and community composition of phytoplankton and periphyton were estimated using standard trichromatic spectrophotometric analysis of Chl *a* (Jeffrey and Humphrey 1975) and high-performance liquid chromatography (HPLC) quantification of biomarker pigments (Leavitt and Hodgson 2001; Steinman et al. 2017), respectively. Briefly, filters were completely extracted with either HPLC-grade acetone (trichromatic Chl *a*) or acetone, methanol, and water in a ratio of 80:15:5 by volume (all pigments and derivatives) for 24 h at −20°C, then filtered (0.2-μm pore membrane) before further processing. HPLC was completed following the standard methods of Leavitt and Hodgson (2001) and following the standard procedures of the Qu'Appelle Valley Long Term Ecological Research (QU-LTER) program (Leavitt et al. 2006; Vogt et al. 2011; Haig and Leavitt 2019). Trichromatic Chl *a* was expressed as μg Chl *a* L^{-1} or μg Chl *a* cm^{-2}, following QU-LTER protocols (Vogt et al. 2011). The ratio of labile Chl *a* to its stable degradation product, pheophytin a, was calculated to evaluate whether pigments represented live material or detritus. As ratios were routinely greater than 15:1 in both phytoplankton (17.01 ± 0.83) and epilithon (17.16 ± 1.04), we assumed that pigments mainly represented metabolically active phototrophs (Leavitt 1993).

Ratios of periphyton to phytoplankton abundance were calculated by dividing volumetric estimates of planktonic pigments by aerial estimates of periphytic biomarkers. This ratio was used to approximate spatial and temporal changes in the relative abundance of primary producers in planktonic and attached habitats. Epilithon were collected from ~50% of Secchi depth at turbid sites (Table 1), therefore it was assumed that the ratio would capture the main changes in relative abundance and composition of the benthic assemblages (Vinebrooke and Leavitt 1999), particularly given the spatial and temporal variation in environmental conditions among sites. This approach may underestimate total phytobenthic response (e.g., episammon and epiepelon; epilithon at transparent sites) relative to a comprehensive, but impractical, analysis of phytobenthos in the 180 field collections.

Hydrometric data

Stream discharge was either directly measured, recorded by gauging stations, or calculated using the drainage area ratio method depending on seasonal flow and site characteristics. At wadeable sites, we calculated instantaneous discharge rate (Q) by summing the product of discrete velocities and their respective cross-sectional areas measured at 10–15 points along an orthogonal transect across the creek, following the two-point and 6/10th methods (Buchanan and Somers 1976). When sites were unwadeable, discharge was calculated from provincial and federal hydrometric gauging stations, or by applying the drainage area ratio method following Swarbrick (2017).

Numerical analyses

We used hierarchical generalized additive models (Pedersen et al. 2019) to quantify spatio-temporal trends in abundance and composition of phytoplankton and periphyton both alone, and in response to variation in in situ physico-chemical conditions or effluent influx. Generalized additive models (GAMs) were used to estimate trends in mean values and estimate uncertainties and are uniquely capable of capturing both linear and non-linear relationships among variables. Trichromatic Chl *a* was used as a proxy for abundance of total phototrophs, while community composition was estimated in GAMs using a suite of biomarker pigments: fucoxanthin (siliceous algae), alloxanthin (cryptophytes), chlorophyll *b* (chlorophytes), and echinenone (total cyanobacteria). Other pigments were not included in the main models either because compounds were rare (e.g., peridinin) or exhibited significant taxonomic overlap with selected biomarkers (e.g., cyanobacterial carotenoids). Additionally, Chl *a* derived from HPLC was modeled for comparison with trichromatic Chl *a*. The Qu'Appelle River site immediately upstream of the Wascana Creek-Qu'Appelle River confluence (site 6, Table 1) was excluded from GAMs but was analyzed separately to better identify the mechanisms contributing to downstream patterns in the Qu'Appelle River.

Spatio-temporal models included a fixed effect of year, marginal smooth terms for day of year (day hereafter) and distance along the stream flow path, plus a smooth interaction for day and distance that allowed estimation of seasonal difference along our lotic continuum (Supporting Information Table S1). Distance and day terms also included a tensor product smooth of year to allow for year-specific effects. Additionally, GAMs of community composition included day and distance factor-smoothers for pigment-specific responses. Preliminary models initially included most physico-chemical parameters as predictive variables, while testing for both instantaneous and lag effects. Due to weak explanatory power, we omitted redundant predictors (turbidity) and time lags but retained effects of distance, day, discharge, pH, dissolved nutrients (NO_3^-, NH_4^+, SRP), the mass ratio of TDN to SRP, Secchi transparency, specific conductance, and temperature. To achieve better dispersion of the data, NO_3^-, NH_4^+, TDN: SRP, turbidity, and specific conductance were $\log_{10}$-transformed, whereas SRP and discharge were square-root transformed. Multi-colinearity among predictors was estimated using Pearson correlation coefficients for all pairs of predictors and concurvity of model smooths; no Pearson correlation was > 0.35, but smoother concurvity was high (0.7–0.9) suggesting non-linear correlation of parameters. To address non-linear correlations and to achieve best fit and parsimony, we penalized the range and null space of the smoothing

matrices for physico-chemical variables during fitting with the option *select* = *true* (Marra and Wood 2011).

All models were run within the R statistical environment (v. 3.6.2; R Core Team 2018) with *mgcv* (v. 1.8–29; Pedersen et al. 2019) package with automatic smoothness estimation (Wood 2011; Wood 2017). Prior to model creation, a redundancy analysis (RDA) was performed with physico-chemical constraints to determine initial linear relationships between pigments and physico-chemical covariates. As RDA axes explained little variance (<20%) and most biologically relevant covariates were removed from the RDA after variable selection using forward selection or backwards elimination, we inferred that that underlying relationships were non-linear in nature. We used a gamma distribution (positive, continuous responses) with a log-link function for Chl *a* models because concentrations were >0 $\mu g\ L^{-1}$. However, because concentration of other biomarker pigments were occasionally below detection limits (<0.002 nmol pigment L^{-1} or cm^{-2}), a Tweedie distribution (zero-inclusive, positive, continuous responses) was used for those models. We did not treat these observations as censored because <1% of values were 0 and likely truly absent (0.0 nmol pigment L^{-1}) and because preliminary analysis with Bayesian regression models using *Stan* (BRMS, v. 2.10.0; Bürkner 2018) greatly overestimated observed pigment concentrations (i.e., exhibited a poor fit relative to *mgcv* models). In addition, models dealt with missing values internally by omitting samples with absent physico-chemical variables.

To analyze changes in community composition, GAMs were developed to include global (all pigments) and pigment-specific smooth terms. This modeling approach allowed us to determine the response of all pigments together as well as isolate how each pigment changed within that main response. Global terms were tensor-product smoothers, whereas pigment-specific terms were factor smoothers (Pedersen et al. 2019). We compared model residuals against physico-chemical parameters to determine which variables required taxa-specific response; all pigment models exhibited a substantial decrease in the magnitude of residuals and better homogeneity when taxa-specific responses were included. We assessed basis size, dispersion of residuals, homogeneity of variance, and the relationship between the observed and predicted response for all models to evaluate whether model assumptions were violated. Residual maximum marginal likelihood (REML) was used for smoothness selection (Wood 2011). Spatio-temporal model predictions and physico-chemical model marginal smooths were visualized in R using *ggplot2* (v. 3.2.1; Wickham 2016).

To quantify the relationship between effluent influx and changes in the abundance and community composition of phototrophic communities, GAMs were developed as above for Chl and biomarker pigments using only $\delta^{15}N$ of filtered water samples, day, and distance from wastewater treatment plant as predictors. Effluent from Regina is highly enriched in ^{15}N isotopes due to nitrification, denitrification and NH_4^+ volatilization, and takes an elevated value (~20–25 ‰) relative to regional background stream values (ca. 5–7 ‰) (Leavitt et al. 2006). This enrichment is evident downstream in filtered water (dissolved N), suspended POM (phytoplankton N), and benthic films (periphyton N) so long as urban N is a significant fraction of the total dissolved N pool (Leavitt et al. 2006). Incorporation of ^{15}N into particulate fractions demonstrates biological update, while elevated values in filtered water illustrate the distance downstream over which effects of effluent may be expected.

Results

Stream conditions

Physicochemical conditions varied substantially from the headwaters of Wascana Creek to the downstream reaches of the Qu'Appelle River in both 2018 and 2019 (Table 1, Fig. 2). Headwaters immediately above the wastewater treatment plant outfall were usually slow-flowing (<1 $m^3\ s^{-1}$), moderately turbid (25–50 NTU; Secchi < 25 cm), alkaline (pH > 8.5), and relatively ion-poor (specific conductance ~1000 $\mu S\ cm^{-1}$), with low concentrations of TDN (<1 mg N L^{-1}) and relatively high levels of P (0.1–0.5 mg P L^{-1}) resulting in low TDN:SRP mass ratios (13.8 ± 2.7) compared to other reaches (Table 1). The presence of Wascana Lake between the two headwater sites resulted in a decline in dissolved P fractions, water transparency, and conductivity, and a modest increase in pH and TDN:SRP ratios.

Influx of urban effluent altered the physico-chemical profile of Wascana Creek and, to a lesser extent, the Qu'Appelle River, with particularly marked effects in 2018 (Fig. 2). Mean ($\pm$ SE) effluent was circumneutral (7.42 ± 0.01 pH) and contained high concentrations of NO_3^- (5.80 ± 0.07 mg N L^{-1}) relative to NH_4^+ (1.82 ± 0.07 mg N L^{-1}) and TDP (0.58 ± 0.02 mg P L^{-1}), with relatively low C:N ratios (4.98 ± 0.11) and strongly enriched $\delta^{15}N$ values (annual mean 16.8 ± 0.3 ‰) (Table 1, Supporting Information Fig. S3). When combined with Wascana Creek streamflow, effluent outfall led to substantial increases in dissolved N concentrations (TDN, NO_3^-, NH_4^+), discharge, and water transparency (increased Secchi depth, reduced turbidity). Further, $\delta^{15}N$ values for filtered Wascana Creek water increased from regional baselines of 3–6 ‰ to 18–23 ‰ in summer (Fig. 2). In contrast, pH declined sharply to ~8, whereas influx of effluent had more limited effects on stream temperature and dissolved P concentrations (Fig. 2). Due to changes in the nutrient regime following effluent outfall, TDN:SRP mass ratios increased to >23:1 (Fig. 2), suggesting either phosphorous limitation of phototrophs or, based on bioassay experiments, saturation of nutrient demands (Supporting Information Fig. S1).

For many parameters (except Q, SRP), effects of effluent influx diminished with distance downstream, with a return to near-headwater conditions near the confluence of Wascana Creek with the Qu'Appelle River (Fig. 2). Discharge

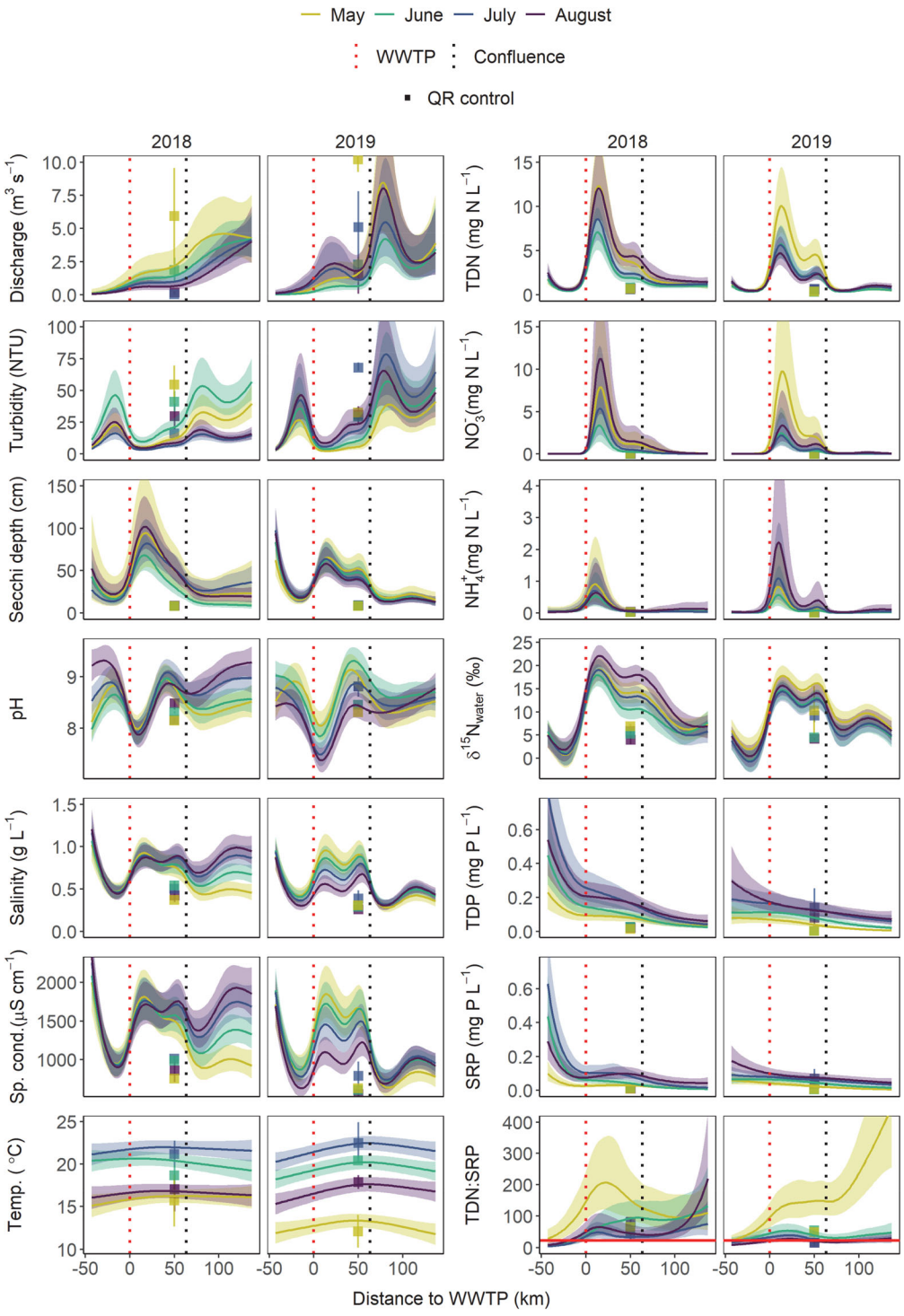

Fig 2. The modeled spatial and temporal distribution of physico-chemical parameters in 2018 and 2019 in Wascana Creek and Qu'Appelle River along a continuum in reference to Regina's wastewater treatment plant (WWTP). Deviance in physical–chemical variables explained by generalized additive models using day of year, distance to wastewater treatment plant, and their interaction as predictors included: Discharge (67.6%), turbidity (82.2% for 2018, 80.0% for 2019), Secchi depth (75.5%), pH (78.4%), salinity (80.1%), specific conductance (77.6%), temperature (87.7%), TDN (87.4%), NO_3^- (79.3%), NH_4^+ (64.6%), $\delta^{15}N$ (83.0%), TDP (70.3%), SRP (78.0%), and TDN:SRP (85.6%). Colored lines are predicted means at four days of year (136, 170, 200, 236) that correspond to summer months in the growing season. Shaded areas are 95% confidence intervals. Square boxes and error bars are the monthly mean and confidence intervals, respectively, of a control site in Qu'Appelle River ~5 km upstream of the Wascana Creek-Qu'Appelle River confluence that was not modeled. Red and black dotted lines represent the inflow of urban effluent into Wascana Creek and the confluence of Wascana Creek with Qu'Appelle River, respectively. The red horizontal line in the TDN:SRP panel is at 23 above which P-limitation occurs.

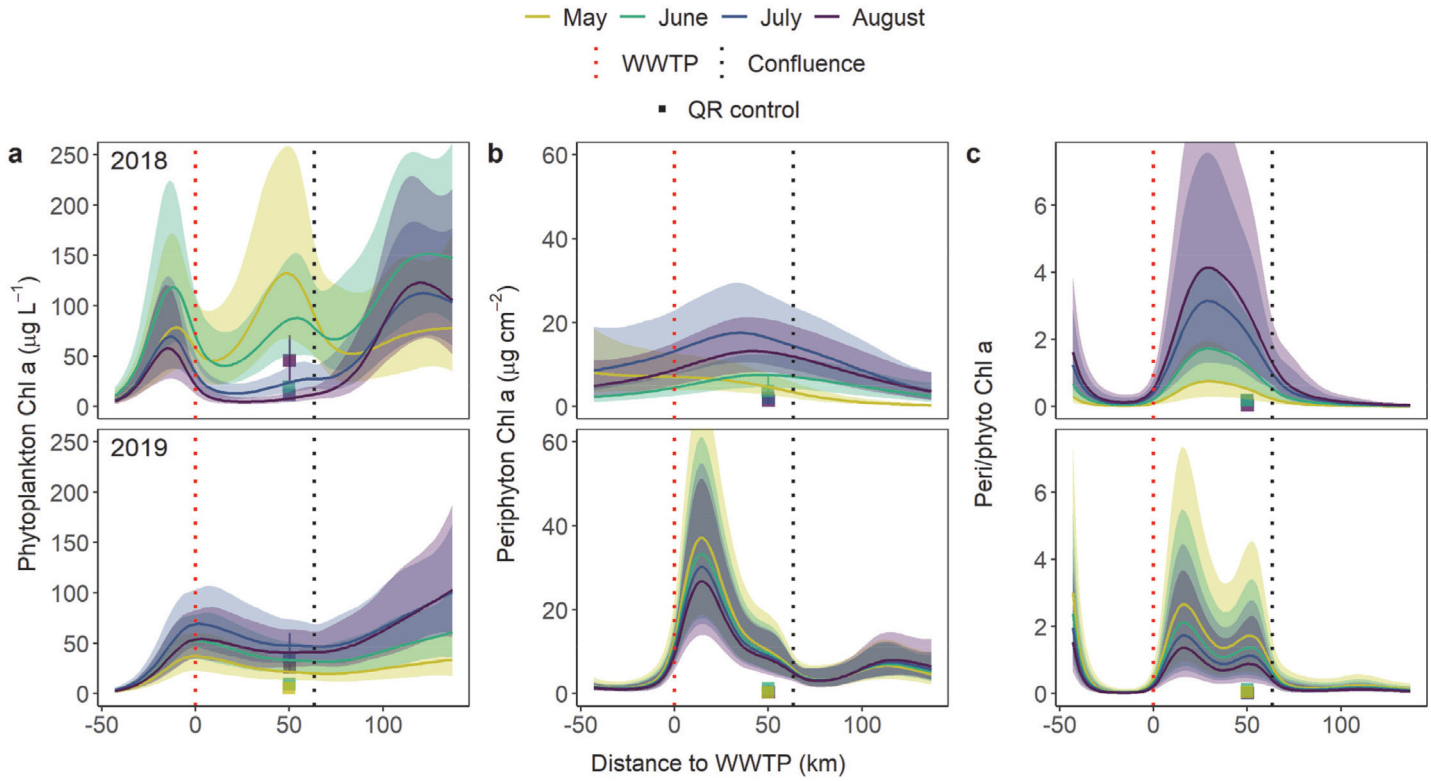

Fig 3. The modeled spatial and temporal distribution of total suspended (phytoplankton, **a**) and benthic (epilithon, **b**) algae and cyanobacteria and their ratio (**c**), using trichromatic chlorophyll *a* as a proxy, in 2018 (top) and 2019 (bottom) in Wascana Creek and Qu'Appelle River along a continuum in reference to Regina's wastewater treatment plant (WWTP). Generalized additive models explained deviance in abundance of phytoplankton (62.6%), epilithon (45.5%) and their ratio (53.9%) using day of year, distance to wastewater treatment plant, and their interaction as predictors. Colored lines are predicted means at four days of year, 136, 170, 200, 236, which correspond to months in the growing season. Shaded areas are 95% confidence intervals. Square boxes and error bars are the monthly mean and confidence intervals, respectively, of a control site in Qu'Appelle River ~5 km upstream of the Wascana Creek-Qu'Appelle River confluence that was not modeled. Red and black dotted lines represent the inflow of effluent into Wascana Creek and the confluence of Wascana Creek with Qu'Appelle River, respectively.

(>2.5 m^3 s^{-1}) and often turbidity (10–60 NTU) reached maximal values in the Qu'Appelle River, water transparency often declined a minimum (Secchi < 20 cm, elevated turbidity), and other parameters (pH, salinity, specific conductivity) returned to background levels. In general, elevated nutrient concentrations and $\delta^{15}N$ values in Wascana Creek waters declined after the Qu'Appelle River confluence, with particularly marked dilution of dissolved N compounds (Fig. 2). Together, these patterns show that most pronounced physico-chemical effects of urban effluent influx were restricted to Wascana Creek in the ~60 km below the wastewater treatment plant.

Landscape regulation of total phototroph abundance

Analysis of trichromatic Chl *a* using GAMs revealed the presence of strong spatial–temporal patterns of primary producer abundance (Fig. 3). Generalized additive model analysis using year, distance, day, and their interaction as predictors explained 62.6%, 45.5%, and 53.9% of deviance in phytoplankton, periphyton, and periphyton:phytoplankton ratios, respectively (Supporting Information Table S1). All predictive terms were significant ($p < 0.05$), except in the ratio model where only distance and day were retained. This analysis suggests that phototrophic communities exhibited marked variation among headwater, effluent-impacted, and post-confluence reaches, as well as significant seasonal variability.

Phytoplankton and epilithon exhibited markedly different spatial patterns of abundance (as Chl *a*) along the continuum formed by Wascana Creek and the Qu'Appelle River (Fig. 3). In both years, total phytoplankton in headwaters increased to a peak downstream of Wascana Lake, declined following receipt of urban effluent, and increased after confluence with the already-turbid Qu'Appelle River (Fig. 3a). In general, phytoplankton patterns were more pronounced during 2018 than in 2019, with GAM analysis revealing significant decreases in Chl *a* associated with wastewater influx in both July and August 2018, but not during May and June 2018. In contrast, periphyton abundance increased sharply after wastewater treatment plant inputs, before decreasing downstream of the confluence (Fig. 3b). In this case, analyses showed that periphyton only increased significantly after the wastewater treatment plant in 2019, while a significant and substantial increase in periphyton:phytoplankton ratios was recorded

downstream of the wastewater treatment plant in both years and all seasons (Fig. 3c). Similar spatial patterns of change were recorded for both phytoplankton and epilithon assemblages when analyzed with Chl *a* quantified using HPLC (Supporting Information Fig. S4).

Analysis of trichromatic Chl *a* using GAMs suggested that landscape patterns of phytoplankton and periphyton abundance were regulated mainly by changes in discharge, transparency, and solute concentrations (Fig. 4). Overall, measured environmental conditions explained 66.3% of deviance in total phytoplankton abundance, and 53.9% in that of total epilithon, with significant effects ($p < 0.05$) of distance downstream (both communities) and DOY (phytoplankton only) (Supporting Information Table S1). Total phytoplankton abundance increased with discharge, specific conductance, and secondarily NH_4^+ concentration, but declined with elevated Secchi depth, NO_3^- levels, and SRP content (Fig. 4a). In contrast, periphyton abundance increased significantly ($p < 0.05$) with NH_4^+ concentrations and declined with elevated discharge and elevated Secchi depth (Fig. 4b). Effects of water temperature and TDN:SRP ratios were not significant ($p > 0.1$) in either habitat (smooth linear and flat, EDF ~ 0), while pH effects where marginal ($p > 0.05$).

Landscape regulation of community composition

Phytoplankton and periphyton assemblages exhibited substantial spatial and temporal variation in community composition (Fig. 5). Landscape position (distance), day, and their interactions explained high proportions of deviance in community composition within GAMs for phytoplankton (86.5%), periphyton (81.1%), and their ratios (77.5%). Both suspended and benthic communities exhibited abundant siliceous algae (as fucoxanthin) at most stations, with additional site-specific contributions from cryptophytes (alloxanthin), chlorophytes (Chl *b*), and total cyanobacteria (echinenone). Further, HPLC analysis revealed that planktonic cyanobacteria routinely consisted of colonial forms (as myxoxanthophyll) in all reaches, whereas periphytic cyanobacteria also included N_2-fixing Nostocales (canthaxanthin) in Wascana Creek headwaters and downstream Qu'Appelle River reaches (Supporting Information Fig. S5).

Spatial variation in the abundance of individual algal and cyanobacterial groups differed among years (Fig. 5). In general, all phytoplankton groups increased between the two headwater stations, before declining markedly downstream of the wastewater treatment plant, particularly in the case of cryptophytes and total cyanobacteria. In contrast, abundance of suspended chlorophytes and siliceous algae increased significantly below the effluent outfall in spring and early summer of 2018. All planktonic groups typically increased downstream of the confluence with the Qu'Appelle River in both years (Fig. 5a). Unlike phytoplankton, all epilithon groups increased significantly in urban-impacted waters in 2019, with more limited increases observed in late summer 2018. Abundance of periphyton usually declined within ~40 km of wastewater outfall and remained low following the confluence of Wascana Creek and Qu'Appelle River, with the exception of

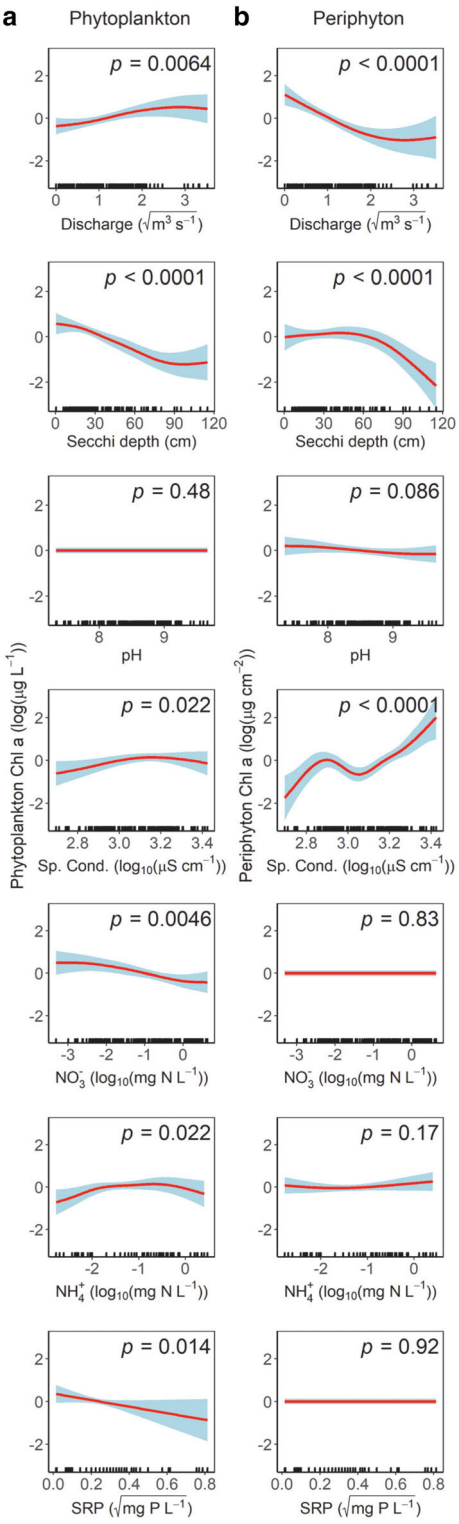

Fig 4. Legend on next page.

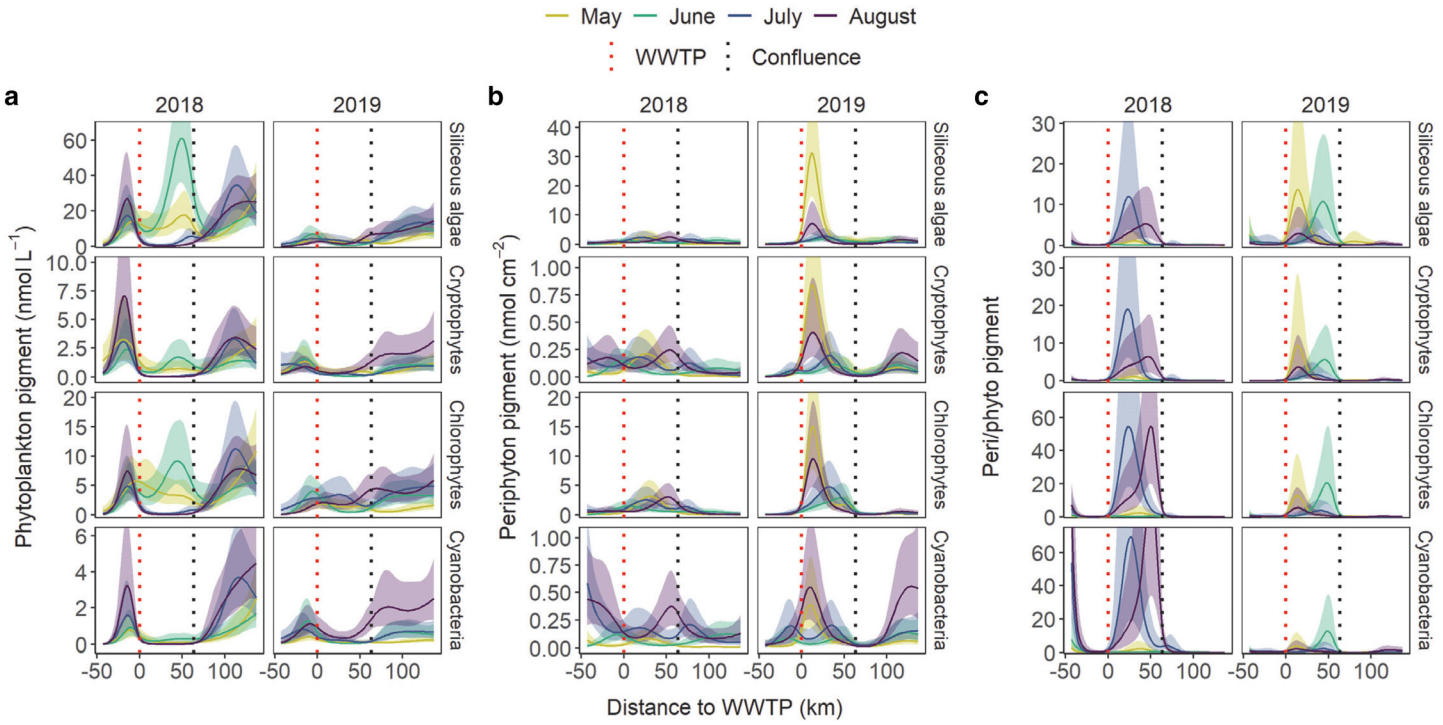

Fig 5. The modeled spatial and temporal distribution of suspended (phytoplankton, **a**) and benthic (periphyton, **b**) algae and cyanobacteria pigments and their ratio (**c**), using pigment biomarkers, in 2018 and 2019 in Wascana Creek and Qu'Appelle River along a continuum in reference to Regina's wastewater treatment plant (WWTP). Modeled taxa by pigment include siliceous algae (fucoxanthin), cryptophytes (alloxanthin), chlorophytes (chlorophyll *b*), and total cyanobacteria (echinenone). Deviance explained by generalized additive models using day of year, distance to wastewater treatment plant and their interaction as predictors of phototroph abundance was 87.0% for phytoplankton, 81.0% for periphyton, and 77.5% for their ratio. Colored lines are predicted means at four days of year, 136, 170, 200, 236, in 2018 and 2019 that correspond to summer months in the growing season. Shaded areas are 95% confidence intervals. Red and black dotted lines represent the inflow of effluent into Wascana Creek and the confluence of Wascana Creek with Qu'Appelle River, respectively.

cryptophytes (Fig. 5b) and diazotrophic cyanobacteria (Supporting Information Fig. S5) which increased in the Qu'Appelle River during 2019. Benthic: planktonic ratios of most phototrophic groups increased immediately downstream of the wastewater treatment plant (Fig. 5); however, timing of changes varied among years, with elevated ratios during July–August in 2018 and May–June in 2019 (Fig. 5). Overall, these patterns suggest that influx of urban effluent favored chlorophytes and siliceous algae in both habitats, while N_2-fixing cyanobacteria were common in Wascana Creek headwaters and Qu'Appelle River locations.

Analysis of landscape patterns of phototroph community composition using GAMs with diverse physico-chemical predictors explained 84.0% of deviance in phytoplankton and 72.6% in periphyton when years were analyzed together (Fig. 6, Supporting Information Table S1) or separately (not shown). For phytoplankton (Fig. 6a), significant global effects ($p < 0.05$; all biomarkers together) were recorded for all chemical (except pH) and physical variables, as well as spatial (distance) and temporal (day) parameters. Similarly, significant taxon-specific effects were included for all variables, except pH (marginal effect) (Fig. 6a). Many physico-chemical parameters also exhibited significant global effects on epilithic assemblages (except temperature, SRP, and, marginally, TDN:SRP), while taxon-specific effects were recorded for all parameters except discharge and, marginally, NO_3^- (Fig. 6b).

Physico-chemical factors had differential effects on phototrophic communities when analyzed at the landscape scale (Fig. 6). Across all sites, high discharge rates favored elevated phytoplankton abundance and reduced densities of

FIG 4. The modeled marginal smooth effects of physico-chemical variables on total phytoplankton (**a**) and periphyton (**b**) biomass (trichromatic Chl *a*) in response to changes in physico-chemical parameters (rows) measured in Wascana Creek and the Qu'Appelle River during May–September 2018 and 2019. Red lines represent the mean effect. Blue-shaded areas are 95% credible intervals. Deviance explained by generalized additive models using physico-chemical parameters, day of year, and distance to wastewater treatment plant as predictors of changes in phytoplankton and epilithon abundance were 66.3% and 53.9%, respectively. *p* values are located at the top of each plot. Temperature and TDN:SRP were nonsignificant (not presented). Turbidity was removed due to covariation with Secchi depth.

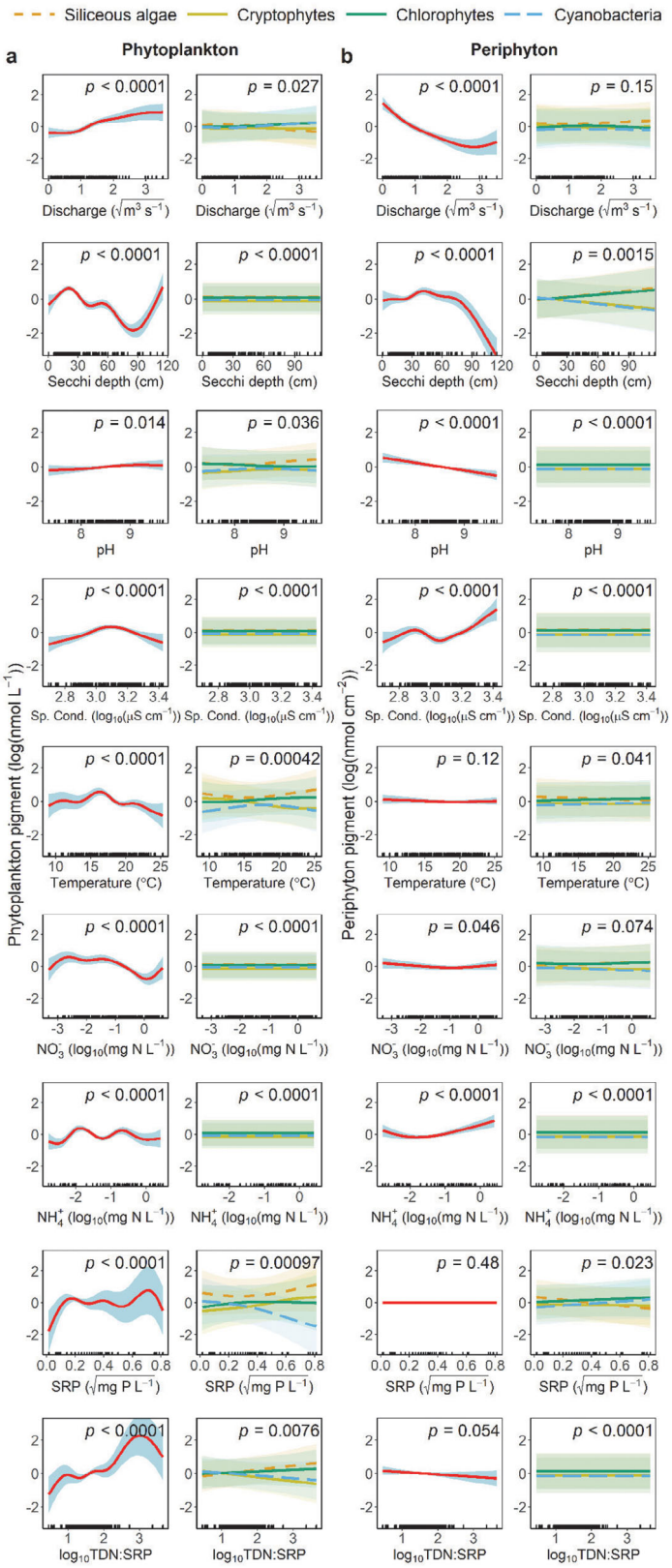

periphyton, but analysis revealed limited effects of community composition in either habitat. Irradiance regime had nonlinear global effects on assemblages (Fig. 6), with marked increases in phytoplankton and declines in periphyton at Secchi depths >90 cm, mainly due to siliceous algae and chlorophytes. Overall, pH had minimal effects on phytoplankton, other than a slight increase in siliceous algae in alkaline conditions, whereas periphyton declined modestly with increased pH due to more pronounced responses of chlorophytes. Both specific conductance and temperature exhibited complex, nonlinear relationships with phytoplankton and periphyton, although in both cases global responses of assemblages were significantly influenced by the presence of chlorophytes and secondarily siliceous algae.

In general, phytoplankton and periphyton assemblages exhibited contrasting relationships to concentrations of dissolved nutrients (Fig. 6). Dissolved N species generally had their greatest global effects on phytoplankton, and a diminished influence on periphyton, at intermediate nutrient concentrations, with elevated effects of chlorophytes or siliceous algae in both habitats. Effects of SRP were indistinct, with pronounced differences in response of siliceous algae and cyanobacteria in both habitats. Global effects of TDN:SRP ratios on phytoplankton increased with the nutrient ratio, whereas effects on epilithon declined, largely reflecting responses of chlorophytes and siliceous algae.

Effects of effluent on phytoplankton and periphyton

Influx of effluent from biological nutrient removal processes was correlated strongly to changes in abundance and composition of phytoplankton and periphyton when analyzed using GAMs with stream-water $\delta^{15}N$, distance from wastewater treatment plant, and day as predictors (Fig. 7). Abundance of phytoplankton as both Chl *a* (51.6% deviance explained) and global response of all biomarkers (67.1%) declined markedly as $\delta^{15}N$ increased from background (ca. 5–7 ‰) values (Leavitt et al. 2006) to those characteristic of nearly pure effluent (20–25 ‰) (Fig. 2). In contrast, total periphyton abundance as either Chl *a* (21.5% deviance explained) or

Fig 6. The modeled marginal smooth effects of physico-chemical variables on phytoplankton (**a**) and epilithon (**b**) biomarker pigments in response to changes in physico-chemical parameters (rows) measured in Wascana Creek and the Qu'Appelle River during May–September 2018 and 2019. Deviance explained by GAMs using indicated physico-chemical parameters, day of year, and distance to wastewater treatment plant as predictors of changes in the phytoplankton and epilithon was 84.0% and 72.6%, respectively. For the global pigment smooths (all pigments included), red lines represent the mean effect and blue-shaded areas are 95% credible intervals. The taxa-specific effects (how specific pigments vary over global effect) are to the right of the global effect panels and shaded areas are 95% credible intervals. Groups include siliceous algae (fucoxanthin; orange), cryptophytes (alloxanthin; yellow), chlorophytes (Chl *b*; green), and cyanobacteria (echinenone; blue). *p* values are located at the top of each plot. Turbidity was removed due to covariation with Secchi depth.

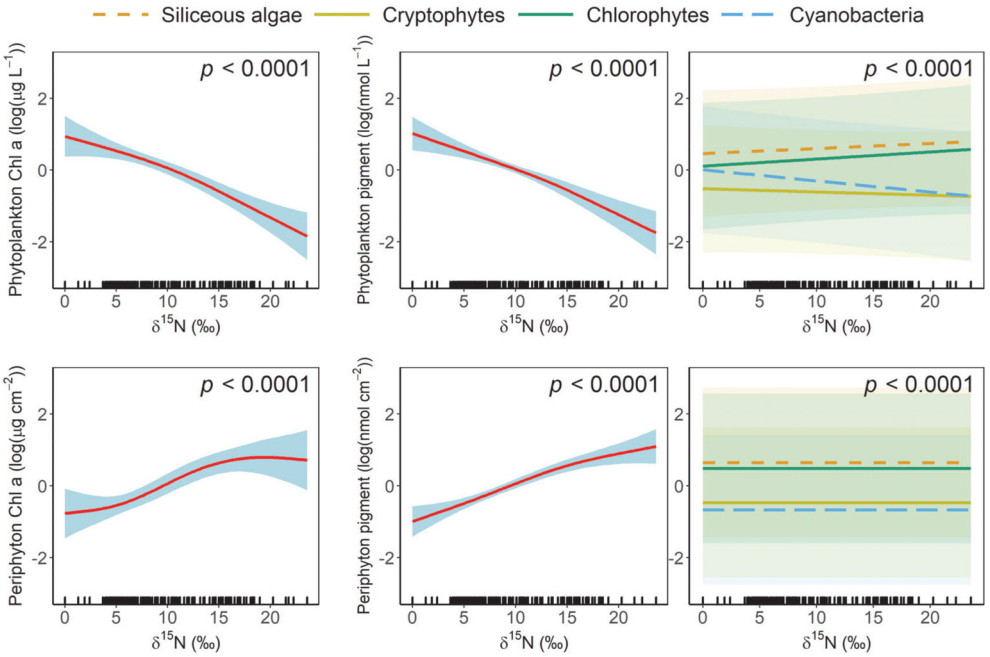

Fig 7. The modeled marginal smooth effects of urban effluent (as $\delta^{15}N_{water}$) on phytoplankton (top row) and periphyton (bottom row) biomass (Chl *a*; left column), global pigment biomarkers (middle column), and taxon-specific effects (right column) in the study area during 2018 and 2019 combined. Red lines represent the mean effect, blue-shaded areas are 95% credible intervals. Generalized additive models using $\delta^{15}N$, distance to wastewater treatment plant, and day of year as predictors were used to explain deviance in phytoplankton abundance (51.6% as Chl *a*) and composition (67.1% as global biomarkers), as well as periphyton abundance (21.5%) and composition (58.8%). All models were highly significant ($p < 0.0001$). Taxon-specific effects (how individual groups vary over the global effect) along with shaded 95% credible intervals are indicated for siliceous algae (fucoxanthin; orange), cryptophytes (alloxanthin; yellow), chlorophytes (Chl *b*; green), and total cyanobacteria (echinenone; blue).

global biomarkers (58.8%) increased with wastewater content in Wascana Creek (Fig. 7). In both habitats, global responses reflect the more pronounced effect of siliceous algae and chlorophytes over cryptophytes and cyanobacteria (Fig. 7).

Discussion

Mechanisms affecting eutrophication of flowing waters can be difficult to discern due to complex interactions between natural and anthropogenic processes (Stevenson and White 1995; Reynolds and Descy 1996; Dodds and Smith 2017), particularly in eutrophic systems (Waiser et al. 2011; Wu et al. 2011; Breuer et al. 2017) or those receiving effluent from advanced wastewater treatment (Carey and Migliaccio 2009; Hamdhani et al. 2020). Here we contrasted the reach-specific effects of effluent produced by biological nutrient removal processes (NO_3^--rich; low NH_4^+, reduced SRP, low turbidity) with landscape effects of natural physico-chemical conditions as controls of phytoplankton and periphyton assemblages in small productive prairie streams. As seen in other eutrophic systems (Leland 2003; Andrus et al. 2015; Breuer et al. 2017; Moorhouse et al. 2018), landscape patterns in abundance and composition of both phytoplankton (66.3%, 84.0% deviance explained, respectively) and periphyton (53.9%, 72.0%) were related mainly to spatial and temporal variation in discharge, water transparency, and solute concentrations (Figs. 4, 6). Unexpectedly, modern urban effluent sharply reduced phytoplankton abundance, while increasing that of periphyton (Figs. 3, 5, 7) and favoring diatoms and chlorophytes over harmful cyanobacteria (Fig. 7), in contrast to responses to wastewater elsewhere (Murdock et al. 2004; Solomon et al. 2019; Hamdhani et al. 2020). Further, use of aqueous $\delta^{15}N$ as a wastewater-specific marker revealed that 39.9–81.7% of landscape deviance in phototrophs could itself be explained by changes in effluent content, mainly within a 60-km reach below the wastewater treatment plant. Analysis with GAMs also suggested that the strong reciprocal changes in phytoplankton and epilithon arose from dilution of turbid stream water with transparent effluent, changes in discharge, and influx of NO_3^- (Figs. 4, 6), the preferred N source for N-limited siliceous algae and chlorophytes (Glibert et al. 2016; Swarbrick et al. 2019). Thus, although natural environmental controls were overwhelmed by wastewater discharge (similar to del Giorgio et al. 1991), influx of urban effluent shifted prairie streams to a clear, biofilm-rich ecosystem state more characteristic of forested (Dodds et al. 2006) or restored habitats (Riley and Dodds 2012).

Phototrophic assemblages in prairie streams

Elevated densities of diverse phytoplankton groups were recorded in both first-order headwaters and larger downstream reaches (Figs. 3, 5; Supporting Information Fig. S5). Similar to other small eutrophic streams (Wu et al. 2011; Breuer

et al. 2017), phytoplankton were abundant in low-order grassland streams, with elevated Chl *a* concentrations (up to 300 μg Chl *a* L^{-1}) greater than those recorded in many large eutrophic rivers (Moorhouse et al. 2018; Varol and Şen 2018). Overall, suspended Chl *a* levels were comparable to values observed previously in regional lakes and rivers (Davies 2006; Waiser et al. 2011; Vogt et al. 2018) and were consistent with measurements in other nutrient-rich and agriculturally influenced temperate streams (Van Nieuwenhuyse and Jones 1996; Wu et al. 2011; Breuer et al. 2017). However, while regional eutrophic lakes that drain into the Qu'Appelle River (Wascana, Buffalo Pound, Last Mountain; Fig. 1) exhibit abundant cyanobacteria during summer (Leavitt et al. 2006; Vogt et al. 2018), including N_2-fixing forms (Donald et al. 2011; Hayes et al. 2019), these small fluvial systems mainly support diatoms and chlorophytes (Fig. 5; Supporting Information Fig. S6) despite regional N limitation of stream phytoplankton (Supporting Information Fig. S1).

Despite abundant phytoplankton, periphyton was well developed in shallow marginal waters throughout the study system (Figs. 3, 5; Supporting Information Fig. S5). These benthic phototrophs respond rapidly to nutrient fertilization (Dodds and Smith 2017) and indicate environmental degradation when Chl *a* exceeds 10–15 μg cm^{-2} (Welch et al. 1988) and filamentous cyanobacteria are common (Peterson and Grimm 1992; Murdock et al. 2004; McCall et al. 2017). Epilithic communities in this study deviated from these expectations in two significant ways. First, while colonial and diazotrophic cyanobacteria were present in attached communities in headwaters and the Qu'Appelle River reaches, particularly during late summer (Supporting Information Fig. S5), associated Chl *a* values rarely exceeded 10 μg Chl *a* cm^{-2} at these locations (Fig. 3). Second, extremely high abundance of epilithon (15–30 μg Chl *a* cm^{-2}) in effluent-influenced reaches were composed mainly of diatoms and secondarily chlorophytes (Fig. 5) rather than cyanobacteria (Murdock et al. 2004). This pattern is also common in urban eutrophic streams where diatoms and *Cladophora* can be co-dominant (Dodds 1991; Hamdhani et al. 2020). Taken together, these observations show that effluent from biological nutrient removal plants can reduce the symptoms of eutrophication by promoting diatom-rich biofilms over colonial cyanobacteria, despite addition of growth-saturating concentrations of N and P.

Abundance and community composition of both phytoplankton and periphyton exhibited complex, nonlinear relationships with measured environmental parameters at the landscape scale (Fig. 2), with particularly marked effects of regional variation in discharge, transparency and some dissolved nutrients (see below), but not temperature or pH (Figs. 4, 6). As seen elsewhere (Murdock et al. 2004), periphyton abundance generally decreased with increasing discharge, with particularly low epilithon abundance at velocities (>1 m s^{-1}) known to induce scouring of benthic habitats (Biggs 1995). While phytoplankton densities may also decline with discharge (Baker and Baker 1979), turbulence-adapted planktonic taxa (diatoms, chlorophytes) actually benefitted from higher flow (Fig. 5; Supporting Information Fig. S5) relative to positively buoyant cyanobacteria (Reynolds and Descy 1996). Overall, the reciprocal relationships between Secchi depth and phytoplankton abundance (Fig. 4), as well as turbidity (not shown), suggests that high densities of suspended algae (see above) were an important factor regulating water column transparency. Because periphyton abundance declined with elevated phytoplankton densities (and turbidity), we infer that shading by suspended algae may have inhibited periphyton growth in headwaters and downstream reaches where Secchi depth was <20 cm (Munn et al. 1989; Rosemond et al. 2000). Similarly, although periphyton abundance was inversely related to Secchi depth (Figs. 4, 6), epilithon only declined at extremely high transparency, possibly due to photoinhibition of diatoms (Schwaderer et al. 2011; Glibert et al. 2016). Although speculative, the absence of substantial effects of temperature and pH (Munn et al. 2002; Wu et al. 2011; Breuer et al. 2017) may reflect the pronounced seasonal increases in both parameters (10°C, 1 pH unit) and the incorporation of associated variance into the day parameter within GAMs. Thus, although experimental research is needed to validate proposed mechanisms, the observation that 73–84% of deviance in both suspended and epilithic communities was explained by measured variables (Fig. 6) suggests that this study identified most key processes regulating regional primary producers.

Effects of modern urban effluent on eutrophic streams

Comparison of the performance of GAMs parameterized with either a comprehensive suite of physico-chemical predictors (Figs. 4, 6) or effluent-specific $\delta^{15}N$ (Fig. 7) demonstrated that up to 80% of explained deviance in the inclusive landscape model was itself attributable to variation in wastewater content of Wascana Creek. Because urban wastewater represents the main source of ^{15}N-enriched dissolved N in the study area (Hayes et al. 2019), elevated $\delta^{15}N$ values in filtered water, phytoplankton, and epilithon (Fig. 2; Supporting Information Fig. S8) can be used to identify influx of effluent N to streams (Leavitt et al. 2006). Whereas phytoplankton in upstream Wascana Creek and the Qu'Appelle River exhibited growth limitation by N in microcosm experiments (Supporting Information Fig. S1), and both suspended and attached communities included N_2-fixing cyanobacteria (Supporting Information Fig. S5), neither N limitation nor N_2 fixation was important in effluent-impacted reaches of Wascana Creek. Instead, phototrophic growth appeared saturated by influx of urban N and P, as seen in other fertilized streams (Van Nieuwenhuyse and Jones 1996; Dodds et al. 2006). Alleviation of N limitation also promoted growth of diatoms and chlorophytes (Figs. 4, 6), as seen in other NO_3^--rich systems (Breuer et al. 2017; Varol and Şen 2018; Solomon et al. 2019) but in contrast to elevated cyanobacteria seen downstream of N-rich tertiary wastewater treatment plants (Kim et al. 2020). Diatoms prefer NO_3^- because of their high nitrate reductase activity (Glibert et al. 2016), abundant NO_3^- transporters, and large intracellular NO_3^--storage vacuoles (Glibert et al. 2016), whereas

chlorophytes tolerate and can be stimulated by high levels of both NO_3^- and NH_4^+ (Glibert et al. 2016; Bogard et al. 2020). In contrast, heterocyteous cyanobacteria are often outcompeted in N-replete waters (Bogard et al. 2020), while nondiazotrophic cyanobacteria prefer chemically reduced N (NH_4^+, urea) over NO_3^- (Glibert et al. 2016; Swarbrick et al. 2019) (Fig. 5). Consistent with prior studies of regional eutrophic lakes, including Wascana Lake (Swarbrick et al. 2020), addition of dissolved P to already P-rich reaches (>50 μg SRP L^{-1}; Fig. 2) had little effect on phototrophic communities beyond a negative association with phytoplankton abundance as Chl *a* (Fig. 4).

Declines in suspended diatoms and chlorophytes with increased $\delta^{15}N_{water}$ values (Fig. 7) and Secchi depth (Fig. 6) suggest that clear urban effluent (~4.5 NTU) diluted turbid (~25 NTU), phytoplankton-rich headwaters, increased water-column transparency (Fig. 2), and expanded epilithic communities, resulting in elevated periphyton:phytoplankton ratios for 40–60 km downstream of the wastewater treatment plant (Figs. 3, 5; Supporting Information Fig. S5). This dilution effect was most pronounced during the latter half of 2018 and early summer of 2019 (Figs. 3, 5), periods when Wascana Creek discharge was composed mainly of urban effluent (Supporting Information Fig. S6). Because periphyton abundance was inversely and significantly related to phytoplankton (and turbidity), we infer that shading by suspended particles may have inhibited periphyton growth in headwaters and downstream reaches (Munn et al. 1989; Rosemond et al. 2000), but that effluent may have alleviated light limitation (Fig. 2). Taken together, our findings show that influx of effluent from wastewater plants using biological nutrient removal altered periphyton:phytoplankton ratios by both reducing densities of suspended phototrophs through dilution and stimulating growth of epilithic diatoms and chlorophytes through provision of light and NO_3^-. However, while wastewater influx suppressed natural mechanisms regulating primary producers as seen with pollution effects elsewhere (del Giorgio et al. 1991; Stevenson and White 1995; Solomon et al. 2019), effects of effluent were themselves transitory, and eutrophic phytoplankton-rich conditions were re-established downstream of the Wascana Creek-Qu'Appelle River confluence because of regional controls (Munn et al. 2002; Black et al. 2010; Andrus et al. 2015).

Conclusions

In this study, influx of urban effluent resulted in an unexpected shift from phytoplankton to periphyton, due to increased water clarity and NO_3^- fertilization. In particular, urban effluent reduced colonial cyanobacteria in both habitats and favored development of siliceous algae and chlorophytes due to multiple mechanisms (Glibert et al. 2016; Solomon et al. 2019; Swarbrick et al. 2019). While influx of effluent overwhelmed natural river flow, irradiance and solute concentrations as controls of primary production in suspended and benthic habitats, landscape analysis also suggested that effects of modern wastewater were limited to a ~60 km interval below the treatment plant outfall and that more typical conditions (Fig. 2) and assemblages (Figs. 3, 5; Supporting Information Fig. S5) were re-established after confluence with the larger Qu'Appelle River (Munn et al. 2002; Black et al. 2010; Andrus et al. 2015). We conclude that wastewater treatment using biological nutrient removal processes is a useful management strategy with clear environmental benefits (Carey and Migliaccio 2009; Holeton et al. 2011), as a turbid, eutrophic stream was transformed into a clearwater ecosystem with rich biofilms of diatoms and chlorophytes, and few harmful cyanobacteria. Such state changes in well documented in shallow lakes (Vadeboncoeur et al. 2003), but rarely observed in small river systems. Further research will be needed in other lotic and lentic systems to evaluation how the importance of effluent from biological nutrient removal processes may vary with the size, productivity, stoichiometry, and catchment characteristics of the receiving water bodies.

References

Andrus, M. J., and others. 2015. Spatial and temporal variation of algal assemblages in six midwest agricultural streams having varying levels of atrazine and other physicochemical attributes. Sci. Total Environ. **505**: 65–89. doi: http://doi.org/10.1016/j.scitotenv.2014.09.033

APHA-AWWA/WEF. 1998. Standard methods for the examination of water and wastewater, 20th ed. Washington, DC: American Public Health Association.

Baker, A. L., and K. K. Baker. 1979. Effects of temperature and current discharge on the concentration and photosynthetic activity of the phytoplankton in the upper Mississippi River. Freshw. Biol. **9**: 191–198. doi:http://doi.org/10.1111/j.1365-2427.1979.tb01502.x

Biggs, B. J. F. 1995. The contribution of flood disturbance, catchment geology and land use to the habitat template of periphyton in stream ecosystems. Freshw. Biol. **33**: 419–438. doi: http://doi.org/10.1111/j.1365-2427.1995.tb00404.x

Black, R. W., P. W. Moran, and J. D. Frankforter. 2010. Response of algal metrics to nutrients and physical factors and identification of nutrient thresholds in agricultural streams. Environ. Monit. Assess. **175**: 397–417. doi:http://doi.org/10.1007/s10661-010-1539-8

Bogard, M. J., R. J. Vogt, N. M. Hayes, and P. R. Leavitt. 2020. Unabated nitrogen pollution favours growth of toxic cyanobacteria over chlorophytes in most hypereutrophic lakes. Environ. Sci. Technol. **54**: 3219–3227. doi:http://doi.org/10.1021/acs.est.9b06299

Breuer, F., P. Janz, E. Farrelly, and K. P. Ebke. 2016. Seasonality of algal communities in small streams and ditches in temperate regions using delayed fluorescence. J. Freshw. Ecol. **31**: 393–406. doi:http://doi.org/10.1080/02705060.2016.1160846

Breuer, F., P. Janz, E. Farrelly, and K.-P. Ebke. 2017. Environmental and structural factors influencing algal

communities in small streams and ditches in Central Germany. J. Freshw. Ecol. **32**: 65–83. doi:http://doi.org/10.1080/02705060.2016.1241954

Buchanan, T. J., and W. P. Somers. 1976. Discharge measurements at gauging stations, p. 1–65.*In* U.S. Geological Survey [ed.], Techniques of water-resources investigations of the United States geological survey—book 3: Applications of hydraulics. United States Government Printing Office.

Bürkner, P. 2018. Advanced Bayesian multilevel modeling with the R package BRMS. R J. **10**: 395–411. http://doi.org/10.32614/RJ-2018-017.

Carey, R. O., and K. W. Migliaccio. 2009. Contribution of wastewater treatment plant effluents to nutrient dynamics in aquatic systems: A review. Environ. Manage. **44**: 205–217. doi:http://doi.org/10.1007/s00267-009-9309-5

Cattaneo, A., and M. C. Amireault. 1992. How artificial are artificial substrata for periphyton? J. N. Am. Benthol. Soc. **11**: 244–256. doi:http://doi.org/10.2307/1467389

Chambers, P. A., D. J. McGoldrick, R. B. Brua, C. Vis, J. M. Culp, and G. A. Benoy. 2012. Development of environmental thresholds for nitrogen and phosphorus in streams. J. Environ. Qual. **41**: 7–20. doi:http://doi.org/10.2134/jeq2010.0273

Davies, J- M. 2006. Application of the Canadian water quality index for assessing changes in water quality along the Qu'Appelle River, Saskatchewan, Canada. Lake Reservoir Manag. **22**: 308–320. doi:http://doi.org/10.1080/07438140609354365

Dodds, W. K. 1991. Factors associated with dominance of the filamentous green alga *Cladophora glomerata*. Water Res. **25**: 1325–1332. doi:http://doi.org/10.1016/0043-1354(91)90110-C

Dodds, W. K., K. Gido, M. R. Whiles, K. M. Fritz, and W. J. Matthews. 2004. Life on the edge: The ecology of Great Plains prairie streams. Bioscience **54**: 205. doi:https://doi.org/10.1641/0006-3568(2004)054[0205:LOTETE]2.0.CO;2

Dodds, W. K., and V. H. Smith. 2017. Nitrogen, phosphorus, and eutrophication in streams. Inland Wat. **6**: 155–164. doi:http://doi.org/10.5268/IW-6.2.909

Dodds, W. K., V. H. Smith, and K. Lohman. 2006. Nitrogen and phosphorus relationships to benthic algal biomass in temperate streams. Can. J. Fish. Aquat. Sci. **63**: 1190–1191. doi:http://doi.org/10.1139/f02-063

Donald, D. B., M. J. Bogard, K. Finlay, and P. R. Leavitt. 2011. Comparative effects of urea, ammonium, and nitrate on phytoplankton abundance, community composition, and toxicity in hypereutrophic freshwaters. Limnol. Oceanogr. **56**: 2161–2175. doi:http://doi.org/10.4319/lo.2011.56.6.2161

Environmental Protection Agency. 2007. Biological nutrient removal processes and costs. Office of Water, Washington, DC. Available from: https://www.epa.gov/sites/production/files/documents/criteria_nutrient_bioremoval.pdf

del Giorgio, P. A., A. L. Vinocur, R. J. Lombardo, and H. G. Tell. 1991. Progressive changes in the structure and dynamics of the phytoplankton community along a pollution gradient in a lowland river—a multivariate approach. Hydrobiologia **224**: 129–154. doi:http://doi.org/10.1007/bf00008464

Glibert, P. M., and others. 2016. Pluses and minuses of ammonium and nitrate uptake and assimilation by phytoplankton and implications for productivity and community composition, with emphasis on nitrogen-enriched conditions. Limnol. Oceanogr. **61**: 165–197. doi:http://doi.org/10.1002/lno.10203

Gücker, B., M. Brauns, and M. T. Pusch. 2006. Effects of wastewater treatment plant discharge on ecosystem structure and function of lowland streams. J. N. Am. Benthol. Soc. **33**: 313–329. doi:https://doi.org/10.1899/0887-3593(2006)25[313:EOWTPD]2.0.CO;2

Haig, H. A., and P. R. Leavitt. 2019. The Qu'Appelle long-term ecological research program: A 26-yr hierarchical platform to study freshwater ecosystems of the northern Great Plains. Limnol. Oceanogr. Bull. **28**: 99–103. doi:http://doi.org/10.1002/lob.10337

Haig, H. A., N. M. Hayes, G. L. Simpson, Y. Yi, B. Wissel, K. R. Hodder, and P. R. Leavitt. 2020. Comparison of isotopic mass balance and instrumental techniques as estimates of basin hydrology in seven connected lakes over 12 years. J. Hydrol. X **6**: 100046. doi:http://doi.org/10.1016/j.hydroa.2019.100046

Hall, R. I., P. R. Leavitt, R. Quinlan, A. S. Dixit, and J. P. Smol. 1999. Effects of agriculture, urbanization and climate on water quality in the northern Great Plains. Limnol. Oceanogr. **43**: 739–756. doi:http://doi.org/10.4319/lo.1999.44.3_part_2.0739

Hamdhani, H., D. E. Eppehimer, and M. T. Bogan. 2020. Release of treated effluent into streams: A global review of ecological impacts with a consideration of its potential use for environmental flows. Freshw. Biol. **65**: 1657–1670. doi:http://doi.org/10.1111/fwb.13519

Hayes, N. M., A. Patoine, H. A. Haig, G. L. Simpson, V. J. Swarbrick, E. Wiik, and P. R. Leavitt. 2019. Spatial and temporal variation in nitrogen fixation and its importance to phytoplankton growth in phosphorus-rich lakes. Freshw. Biol. **64**: 269–283. doi:http://doi.org/10.1111/fwb.13214

Holeton, C., P. A. Chambers, L. Grace, and K. Kidd. 2011. Wastewater release and its impacts on Canadian waters. Can. J. Fish. Aquat. Sci. **68**: 1836–1859. doi:http://doi.org/10.1139/f2011-096

Hutchins, M. G., A. C. Johnson, A. Deflandre-Vlandas, S. Comber, P. Posen, and D. Boorman. 2010. Which offers more scope to suppress river phytoplankton blooms: Reducing nutrient pollution or riparian shading? Sci. Total Environ. **408**: 5065–5077. doi:http://doi.org/10.1016/j.scitotenv.2010.07.033

Jeffrey, S. W., and G. F. Humphrey. 1975. New spectrophotometric equations for determining chlorophylls a, b, c1 and c2 in higher plants, algae and natural phytoplankton.

Biochem. Physiol. Pfl. **167**: 191–194. doi:http://doi.org/10.1016/s0015-3796(17)30778-3

Kim, K., and others. 2020. Nitrogen stimulates *Microcystis*-dominated blooms more than phosphorus in river conditions that favor non-nitrogen-fixing genera. Environ. Sci. Technol. **54**: 7185–7193. doi:http://doi.org/10.1021/acs.est.9b07528

Leavitt, P. R. 1993. A review of factors that regulate carotenoid and chlorophyll deposition and fossil pigment abundance. J. Paleolimnol. **9**: 109–127. doi:http://doi.org/10.1007/BF00677513

Leavitt, P. R., and D. A. Hodgson. 2001. Sedimentary pigments, p. 295–325.*In* J. P. Smol, H. J. B. Birks, and W. M. Last [eds.], Tracking environmental change using Lake sediments. Volume 3: Terrestrial, algal and siliceous indicators. Kluwer. doi:http://doi.org/10.1007/0-306-47668-1_15

Leavitt, P. R., C. S. Brock, C. Ebel, and A. Patoine. 2006. Landscape-scale effects of urban nitrogen on a chain of freshwater lakes in Central North America. Limnol. Oceanogr. **51**: 2262–2277. doi:http://doi.org/10.4319/lo.2006.51.5.2262

Leland, H. V. 2003. The influence of water depth and flow regime on phytoplankton biomass and community structure in a shallow, lowland river. Hydrobiologia **506–509**: 247–255. doi:http://doi.org/10.1023/b:hydr.0000008596.00382.56

Marra, G., and S. N. Wood. 2011. Practical variable selection for generalized additive models. Comput. Stat. Data. An. **55**: 2372–2387. doi:http://doi.org/10.1016/j.csda.2011.02.004

McCall, S. J., M. S. Hale, J. T. Smith, D. S. Read, and M. J. Bowes. 2017. Impacts of phosphorus concentration and light intensity on river periphyton biomass and community structure. Hydrobiologia **792**: 315–330. doi:http://doi.org/10.1007/s10750-016-3067-1

Mischke, U., M. Venohr, and H. Behrendt. 2011. Using phytoplankton to assess the trophic status of German rivers. Int. Rev. of Hydrobiol. **96**: 578–598. doi:http://doi.org/10.1002/iroh.201111304

Moorhouse, H. L., and others. 2018. Characterisation of a major phytoplankton bloom in the River Thames (UK) using flow cytometry and high performance liquid chromatography. Sci. Total Environ. **624**: 366–376. doi:http://doi.org/10.1016/j.scitotenv.2017.12.128

Morin, A., and A. Cattaneo. 1992. Factors affecting sampling variability of freshwater periphyton and the power of periphyton studies. Can. J. Fish. Aquat. Sci. **49**: 1695–1703. doi:http://doi.org/10.1139/f92-188

Munn, M. D., R. W. Black, and S. J. Gruber. 2002. Response of benthic algae to environmental gradients in an agriculturally dominated landscape. J. N. Am. Benthol. Soc. **21**: 221–237. doi:http://doi.org/10.2307/1468411

Munn, M. D., L. L. Osborne, and M. J. Wiley. 1989. Factors influencing periphyton growth in agricultural streams of Central Illinois. Hydrobiologia **174**: 89–97. doi:http://doi.org/10.1007/bf00014057

Murdock, J., D. Roelke, and F. Gelwick. 2004. Interactions between flow, periphyton, and nutrients in a heavily impacted urban stream: Implications for stream restoration effectiveness. Ecol. Eng. **22**: 197–207. doi:http://doi.org/10.1016/j.ecoleng.2004.05.005

Organization for Economic Cooperation and Development 2020. Variable:"Wastewater Treatment". Available from http://stats.oecd.org/Index.aspx?DataSetCode=WATER_TREAT

Pedersen, E. J., D. L. Miller, G. L. Simpson, and N. Ross. 2019. Hierarchical generalized additive models in ecology: An introduction with mgcv. Peerj. **7**: e6876. doi:http://doi.org/10.7717/peerj.6876

Peterson, C. G., and N. B. Grimm. 1992. Temporal variation in enrichment effects during periphyton succession in a nitrogen limited desert stream ecosystem. J. N. Am. Benthol. Soc. **11**: 20–36. doi:http://doi.org/10.2307/1467879

Pham, S. V., P. R. Leavitt, S. McGowan, B. Wissel, and L. I. Wassenaar. 2009. Spatial and temporal variability of prairie lake hydrology as revealed using stable isotopes of hydrogen and oxygen. Limnol. Oceanogr. **54**: 101–118. doi:http://doi.org/10.4319/lo.2009.54.1.0101

R Core Team. 2018. R: a language and environment for statistical computing; https://www.R-project.org/

Reynolds, C. S., and J. -P. Descy. 1996. The production, biomass and structure of phytoplankton in large rivers. River Systems **10**: 161–187. doi:http://doi.org/10.1127/lr/10/1996/161

Riley, A. J., and W. K. Dodds. 2012. The expansion of woody riparian vegetation, and subsequent stream restoration, influences the metabolism of prairie streams. Freshw. Biol. **57**: 1138–1150. doi:http://doi.org/10.1111/j.1365-2427.2012.02778.x

Roeder, D. R. 1977. Relationships between phytoplankton and periphyton communities in a Central Iowa stream. Hydrobiologia **56**: 145–151. doi:http://doi.org/10.1007/bf00023353

Rosemond, A. D., P. J. Mulholland, and S. H. Brawley. 2000. Seasonally shifting limitation of stream periphyton: Response of algal populations and assemblage biomass and productivity to variation in light, nutrients, and herbivores. Can. J. Fish. Aquat. Sci. **57**: 66–75. doi:http://doi.org/10.1139/f99-181

Schindler, D. 1977. Evolution of phosphorus limitation in lakes. Science **195**: 260–262. doi:http://doi.org/10.1126/science.195.4275.260

Schindler, D. W., S. R. Carpenter, S. C. Chapra, R. E. Hecky, and D. M. Orihel. 2016. Reducing phosphorus to curb lake eutrophication is a success. Environ. Sci. Technol. **50**: 8923–8929. doi:http://doi.org/10.1021/acs.est.6b02204

Schwaderer, A. S., K. Yoshiyama, P. d. T. Pinto, N. G. Swenson, C. A. Klausmeier, and E. Litchman. 2011. Eco-evolutionary differences in light utilization traits and

distributions of freshwater phytoplankton. Limnol. Oceanogr. **56**: 589–598. doi:http://doi.org/10.4319/lo.2011.56.2.0589

Solomon, C. M., M. Jackson, and P. M. Glibert. 2019. Chesapeake Bay's "forgotten" Anacostia River: Eutrophication and nutrient reduction measures. Environ. Monit. Assess. **191**: 265. doi:http://doi.org/10.1007/s10661-019-7437-9

Steinman, A. D., G. A. Lamberti, P. R. Leavitt, and D. G. Uzarski. 2017. Biomass and pigments of benthic algae, p. 223–241.*In* F. R. Hauer and G. A. Lamberti [eds.], Methods in stream ecology, v. **1**. Academic press. doi:10.1016/b978-0-12-416558-8.00012-3

Stevenson, R. J., and K. D. White. 1995. A comparison of natural and human determinants of phytoplankton communities in the Kentucky River basin, USA. Hydrobiologia **297**: 201–216. doi:http://doi.org/10.1007/bf00019285

Swarbrick, V. J. 2017. Season impacts and regulation of nitrogen pollutions in the Northern Great Plains: Insights from microcosm, mesocosm, and mensurative-scale studies. PhD thesis. University of Regina. 217 pp.

Swarbrick, V. J., G. L. Simpson, P. M. Glibert, and P. R. Leavitt. 2019. Differential stimulation and suppression of phytoplankton growth by ammonium enrichment in eutrophic hardwater lakes over 16 years. Limnol. Oceanogr. **64**: S130–S149. doi:10.1002/lno.11093

Swarbrick, V. J., Z. Quiñones-Rivera, and P. R. Leavitt. 2020. Seasonal variability in effects of urea and phosphorous on phytoplankton abundance and composition in a hypereutrophic hardwater lake. Freshw. Biol. **65**: 1765–1781. doi:http://doi.org/10.1111/fwb.13580

Tchobanoglous, G., F. L. Burton, and H. D. Stensel. 2003. Wastewater engineering: Treatment and reuse, 4th ed. McGraw-Hill Education, Metcalf and Eddy.

Vadeboncoeur, Y., E. Jeppesen, M. J. V. Zanden, H. Schierup, K. Christoffersen, and D. M. Lodge. 2003. From Greenland to green lakes: Cultural eutrophication and the loss of benthic pathways in lakes. Limnol Oceanogr **48**: 1408–1418. doi:http://doi.org/10.4319/lo.2003.48.4.1408

Van Nieuwenhuyse, E. E., and J. R. Jones. 1996. Phosphorus–chlorophyll relationship in temperate streams and its variation with stream catchment area. Can. J. Fish. Aquat. Sci. **53**: 99–105. http://doi.org/10.1139/cjfas-53-1-99

Varol, M., and B. Şen. 2018. Abiotic factors controlling the seasonal and spatial patterns of phytoplankton community in the Tigris River, Turkey. River Res. Appl. **34**: 13–23. doi:http://doi.org/10.1002/rra.3223

Vinebrooke, R. D., and P. R. Leavitt. 1999. Phytobenthos and phytoplankton as potential indicators of climate change in mountain lakes and ponds: A HPLC-based pigment approach. J. N. Am. Benthol. Soc. **18**: 14–32. doi:http://doi.org/10.2307/1468006

Vogt, R. J., J. A. Rusak, A. Patoine, and P. R. Leavitt. 2011. Differential effects of energy and mass influx on the landscape synchrony of lake ecosystems. Ecology **92**: 1104–1114. doi:http://doi.org/10.1890/10-1846.1

Vogt, R. J., S. Sharma, and P. R. Leavitt. 2018. Direct and interactive effects of climate, meteorology, river hydrology, and lake characteristics on water quality in productive lakes of the Canadian Prairies. Can. J. Fish. Aquat. Sci. **75**: 47–59. doi:http://doi.org/10.1139/cjfas-2016-0520

Waiser, M. J., V. Tumber, and J. Holm. 2011. Effluent-dominated streams. Part 1: Presence and effects of excess nitrogen and phosphorus in Wascana Creek, Saskatchewan. Canada. Environ. Toxicol. Chem. **30**: 496–507. doi:http://doi.org/10.1002/etc.399

Welch, E. B., J. M. Jacoby, R. R. Horner, and M. R. Seeley. 1988. Nuisance biomass levels of periphytic algae in streams. Hydrobiologia **157**: 161–168. doi:http://doi.org/10.1007/bf00006968

Wickham H. 2016. ggplot2: Elegant graphics for data analysis. Springer-VerlagNew York, NY. https://ggplot2.tidyverse.org.

Wood, S. N. 2011. Fast stable restricted maximum likelihood and marginal likelihood estimation of semiparametric generalized linear models. J. Roy. Stat. Soc. B Stat. Methodol. **73**: 3–36. http://doi.org/10.1111/j.1467-9868.2010.00749.x

Wood, S. N. 2017. Generalized additive models: An introduction with R, 2nd ed. Chapman and Hall/CRC.

Wu, N., B. Schmalz, and N. Fohrer. 2011. Distribution of phytoplankton in a German lowland river in relation to environmental factors. J. Plankton Res. **33**: 807–820. doi:http://doi.org/10.1093/plankt/fbq139

Acknowledgments

We thank members of the Limnology Laboratory for assistance with data collection since 2009. We also thank Curtis Hallborg and Trent Wurtz of the Saskatchewan Water Security Agency for data on surface flow in the Qu'Appelle River drainage basin, as well as Kayla Gallant and EPCOR for wastewater information and data, K. Hodder and V. Swarbrick for assistance with discharge calculations, and Zora Quinones-Rivera and D. Bateson for HPLC assistance. This work was supported by the NSERC Canada Discovery Grants program, Canada Research Chairs, Canada Foundation for Innovation, the Province of Saskatchewan, the University of Regina, and Queens University Belfast. We acknowledge that the study sites are on Treaty 4 territory and appreciate the willingness of the Indigenous Peoples of Saskatchewan to protect and share Canada's water resources. This is a contribution of the Qu'Appelle Valley Long Term Ecological Research program (QU-LTER).

Conflict of interest

None declared.

Submitted 24 July 2020
Revised 29 January 2021
Accepted 18 April 2021

Associate editor: Ryan Sponseller